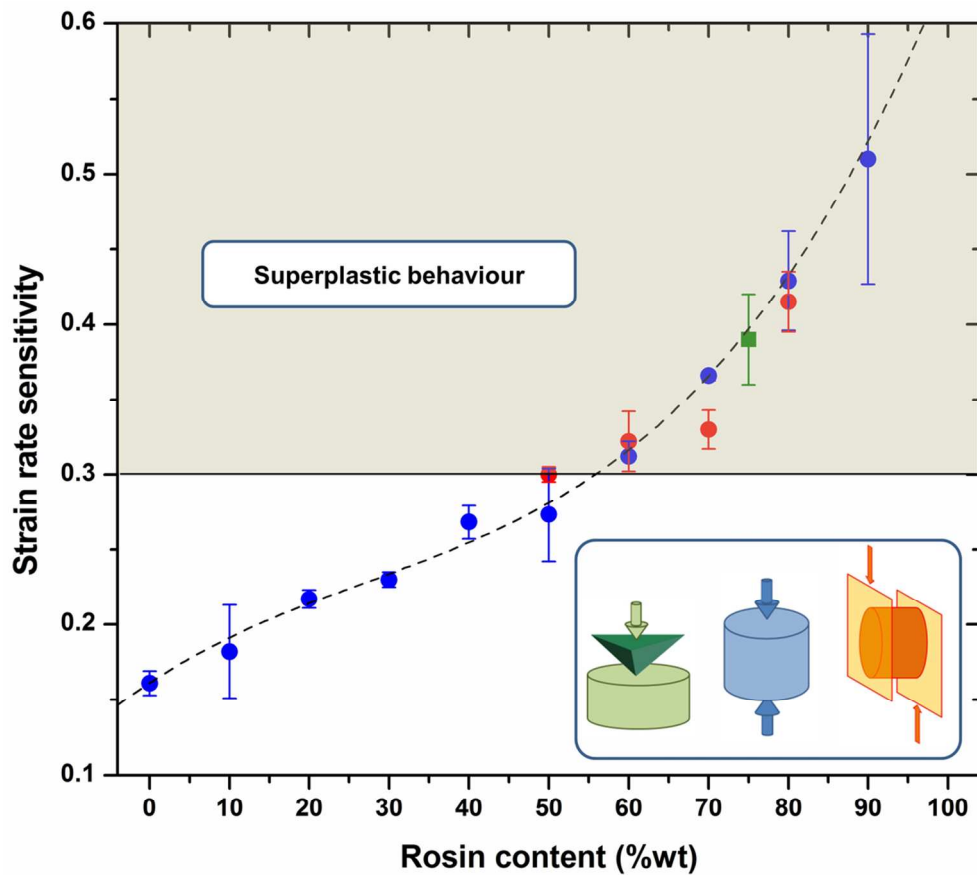


“Superplastic behaviour of rosin/beeswax blends at room temperature.”

Journal:	<i>Journal of Applied Polymer Science</i>
Manuscript ID:	APP-2011-11-4130.R3
Wiley - Manuscript type:	Research Article
Keywords:	adhesives, Biopolymers & renewable polymers, mechanical properties, viscosity and viscoelasticity

SCHOLARONE™
Manuscripts

Peer Review



51x46mm (600 x 600 DPI)

“Superplastic behaviour of rosin/beeswax blends at room temperature.”

Y Gaillard, M. Girard, G. Monge, A. Burr, E. Darque Ceretti, E. Felder.

MINES ParisTech., CEMEF – Centre de Mise en Forme des Matériaux, CNRS UMR 7635, BP 207 1 rue Claude Daunesse 06904 Sophia Antipolis Cedex, France.

Correspondence to: Yves Gaillard (ygaillard@univ-fcomte.fr)

ABSTRACT:

Blends of rosin and beeswax were studied in terms of thermal and mechanical behaviours. Their glass transition and their α relaxation were both characterised either by differential scanning calorimetry (DSC) or by dynamic mechanical and thermal testing (DMTA). This paper is particularly focused on the impact of the microstructure on the mechanical properties studied by compression, shear and nanoindentation tests. It is shown that at room temperature these blends exhibit a viscous behaviour in both elastic and plastic regimes. From these measurements the superplastic behaviour was highlighted for blends having more than 60%wt in rosin. This superplastic behaviour constitutes a real new potential in mechanical reliability of adhesives based on rosin, more generally known for their very brittle behaviour. As a consequence, it should open the way to the design of new shapes.

Keywords: adhesives, biopolymers, superplastic behaviour, mechanical properties, viscoelastic properties.

INTRODUCTION:

Rosin is a bio-sourced material known as a very good “tackifier” due to its very low surface tension when mixed with the correct solvent [1, 2]. However, at room temperature it remains very brittle having toughness in the order of magnitude of tens of $\text{kPa}\cdot\text{m}^{0.5}$, prohibiting most industrial applications in its pristine state. Rosin is at 90% in weight formed by a complex blend of di-terpene based acids with the empirical formula $\text{C}_{20}\text{H}_{30}\text{O}_2$. The other 10%wt are a blend of esters, alcohols, aldehydes and hydrocarbons [2]. Numerous isomers belonging to three acids groups, namely abietic, D-pimaric and labdanic compose the acidic fraction [3, 4]. The cohesion of rosin is ensured by weak bonds (van der Waals interactions and hydrogen bonding of the hydroxyl groups) [5] but the structure remains amorphous as long as one of the isomer does not exceed 30% [6]. The mechanical behaviour of amorphous materials has been extensively studied but none complete bibliography about mechanical properties of rosins was found. Deformed close to their glass transition

temperature (T_g) or under a high confining pressure, amorphous materials can present several deformation mechanisms of plasticity before fracture [7, 8]. At high T/T_g ratio, amorphous materials exhibit a homogeneous Newtonian behaviour. On the other hand when the temperature is much lower than T_g , shear bands are the seat of inhomogeneous deformations. Several deformation mechanisms have been proposed to explain this latest behaviour. Indeed, silica glasses deform by permanent densification and sliding [9, 10]. On the contrary, the plastic deformations of metallic glasses are the result of a collective rearrangement of sheared clusters, i.e. the so-called “shear transformation zone” proposed by Argon [11-13]. A similar concept of sheared micro-domains is also used by Perez for modelling the behaviour of amorphous polymers [14].

One classical way to change mechanical properties, or any other, of polymers consists in blending it with another material or by the incorporation of particles [15-17]. This addition confers to the blends new combined properties, and may modify in the same way, the glass transition temperature and so the rheological properties. Depending on the miscibility of the two initial materials, this blend may result in a homogeneous material with a single glass transition or in a composite one with two glass transitions. In this paper, we will present the study of the thermomechanical behaviour of melted rosin with a bio-sourced plasticizer: beeswax [18]. If the major expected effect of this addition is evidently to improve the toughness of rosin, we will show that it reveals also the superplastic behaviour of some of the obtained blends depending on the beeswax ratio. First, beeswax and rosin in their pristine states but also a blend of rosin and beeswax are studied by step scan DSC in order to characterise fully their polymorphic transitions, glass transitions and melting behaviour. In particular, a close relation between rosin content and polymorphic transition temperatures of the crystalline part of the blend is confirmed. Then the discussion will be devoted to the viscoelastic properties studied by dynamic mechanical analysis in temperature (DMTA). In particular, both glass transition and polymorphic transitions of the different blends appear to be closely related to their viscoelastic behaviour. The last part will be focused on the mechanical properties of the different blends. Particularly, the mechanical responses experienced under different solicitations of compression, shear and nanoindentation, will be compared in terms of strain rate sensitivity. It reveals a viscoplastic behaviour at room temperature which tends to superplasticity for blends containing more than 60%wt of rosin.

MATERIALS AND METHODS:

Pristine rosin and beeswax were both purchased at a professional apiarist [19]. They were melted at 100 °C. The complete melting procedure has been described in a previous paper [18]. The blends are referenced as X%wt where X is the weight proportion of rosin.

Differential scanning calorimetry (DSC) experiments were conducted on a Perkin Elmer 8000. In order to obtain a complete separation between glass and polymorphic transitions [20-24], step scan DSC experiments were performed. A first ramp has been realised to reach complete melting and then the samples are cooled until 0°C. The sample is then re-heated until 80°C. [This is this second heating that is always presented as step scan DSC thermograms in the paper. Step scan consists in incrementing step by step the temperature \(in our case steps of 1.5°C were applied\). Each step is composed of a temperature ramp, where the temperature is increased very rapidly \(40°C/min\), followed by a](#)

[plateau of 45s. In this way, the transitions coming from kinetic processes, like phase transition or melting, are separated from the total heat flow. This method is classically used to isolate phase transitions \(detected during the plateau\) from glass transition \(detected during the temperature steps\) \[25-27\]. In the following, two curves will be presented for each step scan. The “heat flow” curve is representative of glass transition phenomena whereas the “specific heat” curve representative of the total heat flow.](#)

Dynamic mechanical testing in temperature (DMTA) were realised on a Bohlin Instruments apparatus. Cylindrical samples of 8 mm in diameter and 8 mm height were tested in compression. A single temperature ramp between 0 and 60 °C has been applied at a rate of 0.3°C/min. Small deformations of $1.25 \cdot 10^{-4}$ were applied at different frequencies f between 0.1 and 10 Hz. Storage modulus E' , loss modulus E'' but also phase $\tan \delta$ were measured. Strain rate sensitivity m was determined as follows:

$$m_{DMTA} = \frac{d \log E'}{d \log f} \quad (1)$$

Compression and shear tests were performed with an electromechanical Erichsen apparatus at a temperature of 19.8 ± 0.3 °C. Cylindrical samples of 10 mm height and 8 mm in diameter were compressed at constant velocities of 0.0015, 0.01, 0.1, and 1 mm/s. Experiments at constant strain rate were also conducted on 30 and 80 %wt blends. A release agent was used between the sample and the plates of the machine to reduce friction. The friction is considered negligible and the tests are considered purely uniaxial. True stress, σ , and true strain, ε , were defined classically as followed:

$$\sigma = \frac{F}{S(t)} \quad (2) \text{ and } \varepsilon = \ln \left(\frac{l(t)}{l_0} \right) \quad (3)$$

where F is force applied on the sample, l_0 is the initial height of the sample, $l(t)$ the height of the sample measured in-situ during the compression test and $S(t)$ the in-situ section of the sample, calculated from $l(t)$ assuming a volume conservation. The length of the sample is recorded in-situ using a digital camera at an image acquisition frequency of 33 Hz.

Stress-strain curves were fitted following a G'Sell and Jonas law [28], in order to determine the strain rate sensitivity m_{comp} of the different blends. The following law has been used:

$$\sigma = \sigma_0 e^{h_g \varepsilon^u} \dot{\varepsilon}^m \quad (4) \text{ and } m_{comp} = \frac{d \log \sigma}{d \log \dot{\varepsilon}} \quad (5)$$

where σ_0 is the strength, $\dot{\varepsilon}$ is the strain rate \dot{l}/l (where \dot{l} is $\frac{dl}{dt}$) and h_g and u the parameters characteristic of the strain hardening.

Blends were also deformed by shear way as follows. Two pieces of wood were assembled with an adhesive pad cast in an O-ring of 2 mm width and 10 mm diameter. Wood is used to ensure a good adhesion and transfer the shear displacement to the adhesive pad. Global equivalent stress, τ , global equivalent strain, γ , curves were deduced from the following formulae:

$$\tau = \frac{F}{S} \text{ and } \gamma = \frac{\Delta l}{e} \text{ and } m_{shear} = \frac{d \log \tau}{d \log \dot{\gamma}}$$

where S is the section of the adhesive pad, e its thickness, Δl is the relative displacement between the two pieces of wood along the loading direction and $\dot{\gamma} = \dot{\Delta l} / e$ is the global equivalent strain rate.

Nanoindentation tests were realised using an Hysitron apparatus with a Berkovich indenter having a tip defect of about 200 nm radius. Constant \dot{h}/h , where h is the indentation depth and \dot{h} is $\frac{dh}{dt}$, was applied. Calibration of the indenter shape was performed using fused silica as reference. Strain rate sensitivity was determined as follows:

$$m_{nano} = \frac{d \log F|_h}{d \log(\dot{h}/h)} \quad (6)$$

where $F|_h$ is the applied force at constant penetration depth.

RESULTS AND DISCUSSION:

Microstructure:

Microstructures of the different blends were studied in a previous paper [18]. Beeswax is a partially crystalline material. It crystallises following a needle-shaped structure. When mixed with rosin its microstructure evolves and above all the size of the needles decreases. Furthermore, for blends containing up to 90 %wt of rosin, the beeswax fraction consists in spherical crystallites uniformly distributed in the matrix [18]. Pure beeswax exhibits several polymorphic transitions before its melting point at about 65 °C. Studied by DSC, these polymorphic transitions appear clearly at a rate of 1 °C/min [18]. [Figure 1 presents the step scan DSC thermograms obtained for both beeswax and rosin. In case of beeswax, three polymorphic transitions, \$t_1\$, \$t_2\$ and \$t_3\$ before melting \$m\$ are reported in the literature \[22-24\]. All these transitions can be observed on the “specific heat” curve presented on figure 1. In the same time, the “heat flow” curve presents a monotonous increase which confirms that these transitions are not glassy ones. Concerning rosin, the variation in the “specific heat” curve is also observed but around a temperature of 40°C. The amplitude of this variation is very much lower compared to the peaks observed in beeswax. Furthermore, as for beeswax, this variation is not accompanied by any sudden change in the “heat flow” curve. Unlike to ambers and aged or commercialised resins which generally exhibit a glass transition between 20-100°C \[20\], the rosin used here does not exhibit glass transition.](#)

The same experiment has been repeated on a blend of 75%wt in rosin. As it was described elsewhere [18], the addition of rosin in beeswax plays a key role in the polymorphic transitions and their associated temperature. Meanwhile beeswax exhibits three polymorphic transitions in its pristine state during melting, blends containing more than 15%wt in rosin suffer only than two transitions, respectively the t_2 and t_3 transitions. Furthermore, the temperatures associated with t_2 and t_3 appear to decrease with the content of rosin. The beeswax/rosin phase diagram presented in [18] shows that the temperature of the t_2 transition varies from 51°C for pure beeswax to about 33°C for blend containing 90%wt of rosin. For a 75%wt blend, $t_2=38.3^\circ\text{C}$ and $t_3=46.7^\circ$ can be deduced. These values are in good accordance with the thermogram given in figure 2. Additionally, one can observe that blending beeswax with rosin leads to the observation of a glass transition (T_g) characterised by a C_p jump on the “heat flow” curve. T_g has been measured as the inflection point of ΔC_p at a temperature of about 31°C.

Finally, the microstructure of the blends can be understood as follows. As it is shown in [18], blends exhibit a crystalline part uniformly dispersed in the amorphous fraction. The crystals adopt a needle shape, typical feature of beeswax microstructure [29]. The amorphous part comprises the rosin and the amorphous fraction of beeswax. The amorphous fraction of beeswax includes the longest carbon chains, i.e. the molecules of beeswax, typically polyesters that contain up to 95 carbons. The apparition of a glass transition suggests that amorphous parts of beeswax and rosin are intimately linked.

Dynamic mechanical analysis:

The following is devoted to the dynamic mechanical analysis of the different blends. A 75%wt blend was chosen to illustrate the impact of the glass transition and the polymorphic transition on the mechanical properties. Figure 3 presents the evolution of the storage modulus, E' , the phase, $\tan\delta$, and the strain rate sensitivity, m_{DMTA} , as a function of the temperature. For convenience the temperature associated with the glass transition, and the transitions t_2 and t_3 of this blend are also indicated on figure 3. The evolution of the calculated strain rate sensitivity is very similar to the one of $\tan\delta$, measured experimentally.

Typically, one can describe the evolution with the temperature of the thermomechanical response of this blend in the elastic deformation range in the following manner. By DSC (figure 2) T_g is measured at 31°C, the t_2 transition at about 38°C and the t_3 at about 46°C. The complete process, glass transition, polymorphic transition and melting, starts at about 24°C to finish at 60°C. Mechanically, a first increase of $\tan\delta$ and m_{DMTA} is detected between 12 and 35°C. In this range of temperature two distinct phenomena are concerned. First, the glass transition of the blend located at 31°C, and secondly the t_2 transition centered at 38°C, i.e. above 35°C, but starting at about 24°C as shown on figure 2. So, mechanically it appears to be difficult to deconvolute T_g from t_2 . Even so, these two transitions result in a single increase of $\tan\delta$ and m_{DMTA} . A second increase of m_{DMTA} is observed from a temperature of about 40°C, coinciding with the t_3 transition. According to Kameda [22, 24], the polymorphic transitions in beeswax are also accompanied by a mobility in the conformational transformations from a trans-gauche to a trans-trans conformation. This trans-trans conformation

corresponds to the molecular disentanglement and so can be considered as the α relaxation of the beeswax fraction contained in the blends.

It is interesting to note that even at room temperature ($RT=20^{\circ}\text{C}$) the strain rate sensitivity is clearly influenced by the T_g and the t_2 transitions even if these transitions take place respectively at 31 and 38°C . This influence will grow up as well as the t_2 transition will be close to the RT , i.e. as well as the proportion of rosin contained in the blend is going to increase. So, in this way the strain rate sensitivity should increase with the content of rosin.

Superplastic behaviour:

Compression but also shear tests were performed on all the blends. Figure 4 presents the typical stress-strain curves obtained in compression for the 30%wt and for shear tests on the 80%wt. The compression tests presented on figure 4a were realised at constant strain rate of $9.4 \cdot 10^{-4}$, $4.5 \cdot 10^{-3}$, $8.6 \cdot 10^{-3}$, $4.4 \cdot 10^{-2}$ and $8.1 \cdot 10^{-2} \text{ s}^{-1}$. The experimental compression curves are superimposed with the fit of G'Sell-Jonas obtained from equation (4). From the experimental curves a strain rate sensitivity of 0.24 ± 0.01 was deduced from equation (5). Furthermore for the 30%wt, strain softening, characteristic of the mechanical behaviour of beeswax [30], is observed. This softening persists until a rosin percentage of 70%wt. For higher content of rosin, both shear and compression tests exhibit a strain hardening behaviour as shown on figure 4b.

Nanoindentation tests were performed on a 75%wt specimen but also as reference on pristine rosin. Figure 5a presents the force-penetration curves obtained on the 75%wt for different constant values of \dot{h}/h , respectively 4, 0.4, 0.04 and 0.004 s^{-1} . In particular, the unloading curve reveals a viscoplastic behaviour characterised by the nose effect observed above all at high deformation rate [29], revealing that the sample is still plastically deformed while the load is withdrawn. This nose effect can be avoided by interposing between loading and unloading a break of several seconds by holding a constant force [32]. Furthermore, the adhesion between the indenter and the beeswax/rosin blends leads to the measurement of negative forces at the end of the unloading segment. This type of curve is characteristic of indentation on adhesive material [31, 33]. The amplitude of this adhesive force is directly related to the surface of the contact between the tip and the sample when the maximum load is reached.

The obtained indentation curves indicate clearly a high strain rate sensitivity, which is evaluated to 0.39 ± 0.03 using equation (6). Concerning pristine rosin, the indentation curves shown on figure 5b exhibit multiple pop-in events characteristic of very brittle behaviour, but above all do not show any strain rate dependency.

Finally, the strain rate sensitivity was calculated for each mechanical test as indicated in part 2. The values are summarised in figure 6. The one obtained by nanoindentation for the 75%wt appears to be completely in accordance with the ones obtained by compression and shear. The strain rate sensitivity m increases with the rosin contained in the blend until a value of 0.5. According to [34], the mechanical behaviour of the blends can be considered as superplastic for any value of m greater than 0.3, i.e. for a rosin content up to 60 %wt.

SUMMARY AND CONCLUSIONS:

Blends of rosin and beeswax form a partially crystalline material. If the crystalline part is only due to beeswax, the amorphous part is a close blend of rosin and the amorphous part of beeswax. Both amorphous and crystalline parts are decoupled in step scan differential scanning calorimetry. It means that the thermograms exhibit both a glass transition and the α relaxation of beeswax, and this conclusion is confirmed by DMTA measurements.

Strain rate sensitivity at room temperature in the elastic but also in the plastic regime appears to be greatly influenced by the glass transition but also by the first phase transition of the crystalline part of the blends, themselves depending of rosin content. It results that, while in their pristine state beeswax and rosin are two materials which elastic/plastic regimes do not exhibit high strain rate sensitivity at room temperature, blend of rosin and beeswax are more prone to viscous behaviour.

In particular, the viscoplastic behaviour can reach the superplastic regime for blends having more than 60% in weight of rosin. It is interesting to note that the addition of only 10% of plasticizer is enough to enhance the superplastic regime of the rosin. New perspectives for the design of complexe shapes may be exploited thanks to this superplastic behaviour. The mechanical reliability of these adhesives based on rosin will then be largely improved.

Finally, the use of several mechanical tests combined with DSC and DMTA measurements has allowed understanding fully the behaviour of the different blends. Indeed, the complex plastic behaviour of the pristine rosin can not be studied using solely classic mechanical testing. Only the solicitation of the sample under high confining pressures as reached in nanoindentation allows to deform plastically rosin at room temperature. The results given by the different techniques are in good accordance and clearly confirm the superplastic behaviour of beeswax/rosin blends at room temperature.

ACKNOWLEDGEMENTS

The authors would like to acknowledge Dr. Alice Mija and Pr. Nicolas Sbirrazzuoli from the University of Nice-Sophia Antipolis for fruitful discussions about DSC thermograms.

REFERENCES

- [1] Maiti S. Sinha Ray S., Kundu A.K., *Prog. Polym. Sci.*, **14** (1989) 297-338.
- [2] Comin J., *Int. J. Adhesion and Adhesives*, **15** (1995) 9-14.
- [3] Candy L., "Etude des conditions de synthèse et des propriétés d'ASA d'esters d'huiles végétales – Application à l'industrie papetière", PhD dissertation, Institut National Polytechnique de Toulouse, 2003.
- [4] Georgi E.A., *Journal of Chemical Education* (July 1933) 415-418.
- [5] Pilato L., *Phenolic Resins: A Century of Progress*, Springer, 2010.
- [6] Baldwin D.E., Loeblich V.M., Lawrence R.V., *Industrial and Engineering Chemistry*, **3** (2) (1958) 342-346.

- [7] Vandembroucq D., Deschamps T., Coussa C., Perriot A., Barthel E., Champagnon B., Martinet C., *J. of Phys. Cond. Mat.*, **20**, 48 (2008) 485221.
- [8] Perriot A., Martinez V., Grosvalet L., Martinet Ch., Champagnon B., Vandembroucq D., Barthel E., *J. Am. Ceram. Soc.*, **89**, 2 (2006) 596-601.
- [9] Barton J., Guillemet C., *Le verre, science et technologie*, EDP Science, 2005.
- [10] Kermouche G., Barthel E., Vandembroucq D., Dubujet Ph., *Acta Materialia*, **56**, 13 (2008) 3222-3228.
- [11] Argon A.S., *Acta Metallurgica*, **27**, 1 (1979) 47-58.
- [12] Schuh C.A., Hufnagel T.C., Ramamurty U., *Acta Materialia*, **55**, 12 (2007) 4067-4109.
- [13] Gravier S., "Comportement mécanique des verres métalliques massifs – effet d'une cristallisation partielle" PhD dissertation, Institut National Polytechnique de Grenoble, 2006.
- [14] Perez J., *Matériaux non cristallins et science du désordre*, Presses polytechniques et universitaires romandes, 2001.
- [15] Anuar H., Zuraida A., *Composites: part B*, **42** (2011) 462-465.
- [16] Kobayashi T., Wood B., Takemura A., *Journal of Applied Polymer Science*, **119**, (2011) 2714-2724.
- [17] Li J., Wang S., Yang W., Xie B., Yang N., *Journal of Applied Polymer Science*, **121**, (2011) 554-562.
- [18] Gaillard Y., Mija A., Burr A., Darque-Ceretti E. Felder E., Sbirrazzuoli N., *Thermochimica Acta*, **521**, 1-2 (2011), 90-97.
- [19] <http://ets-leygonie.net/>
- [20] Jablonski P., Golloch A., Borchard W., *Thermochimica Acta*, **333**, (1999) 87-93.
- [21] Lee C.M., Lim S., Kim G.Y., Kim D., Kim D.W., Lee H.C., Lee K.Y., *Biotechnology and Bioprocess Engineering*, **9** (2004) 476-481.
- [22] Kameda T., *J. Phys. D: Appl. Phys.*, **38** (2005) 4313-4320.
- [23] Kotel'nikova E.N., Platonova N.V., Filatov S.K., *Geology of Ore Deposits*, **49** (8) (2007) 697-709.
- [24] Kameda T, Tamada Y., *International Journal of Biological Macromolecules*, **44** (2009) 64-69.
- [25] [Pielichowski K, Flejtuch K, Pielichowski J, *Polymer*, **45** \(2004\) 1235-1242](#)
- [26] [Gunaratne L.M.W.K., Shanks R.A, *European Polymer Journal*, **41** \(2005\) 2980-2988.](#)
- [27] [Papageorgiou G.Z., Achilias D.S., Karayannidis G.P., Bikiaris D.N., Roupakias C., Litsardakis G. , *European Polymer Journal*, **42** \(2006\) 434-445.](#)
- [28] G'Sell C., Jonas J., *Journal of Material Science*, **14** (1979) 583-591.
- [29] Schoening F.R.L., *South African Journal of Science*, **76** (1980) 262-265.
- [30] Morgan J., Townley S., Kemble G., Smith R., *Material Science and Technology*, **18**, (2002) 463-467.
- [31] Giri M., Bousfield D.B., Unertl W.N., *Langmuir*, **17** (2001) 2973-2981
- [32] Ebenstein D.M., Pruitt L.A., *Nanotoday*, **1**, 3 (2006) 26-33.
- [33] Yang F., *J. Phys D: Applied Physics*, **35** (2002) 2614-2620.
- [34] Blandin J-J., Suery M., Superplasticité, *Technique de l'ingénieur – Traité matériaux métallique Article M613*, 1996.

Figure captions

Figure 1: Step scan DSC thermograms obtained for beeswax and rosin. t_1 , t_2 and t_3 are the polymorphic transitions of beeswax.

Figure 2: Step scan DSC thermogram obtained for a blend of 75%wt in rosin. t_2 and t_3 are the polymorphic transitions of the crystalline part. T_g refers to the glass transition temperature of the amorphous part.

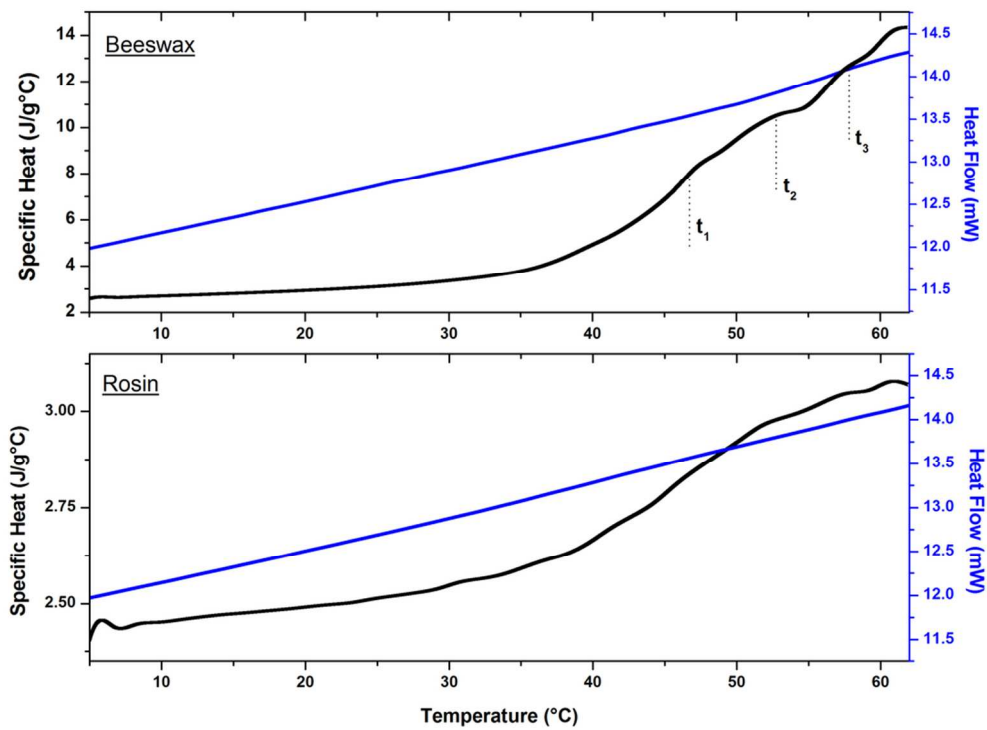
Figure 3: Storage modulus, $\tan \delta$ and strain rate sensitivity m_{DMTA} obtained by DMTA in compression in the 75%wt blend.

Figure 4: Stress-strain curves obtained in compression mode for the 30%wt blend (a) and in shear mode for the 80%wt blend (b).

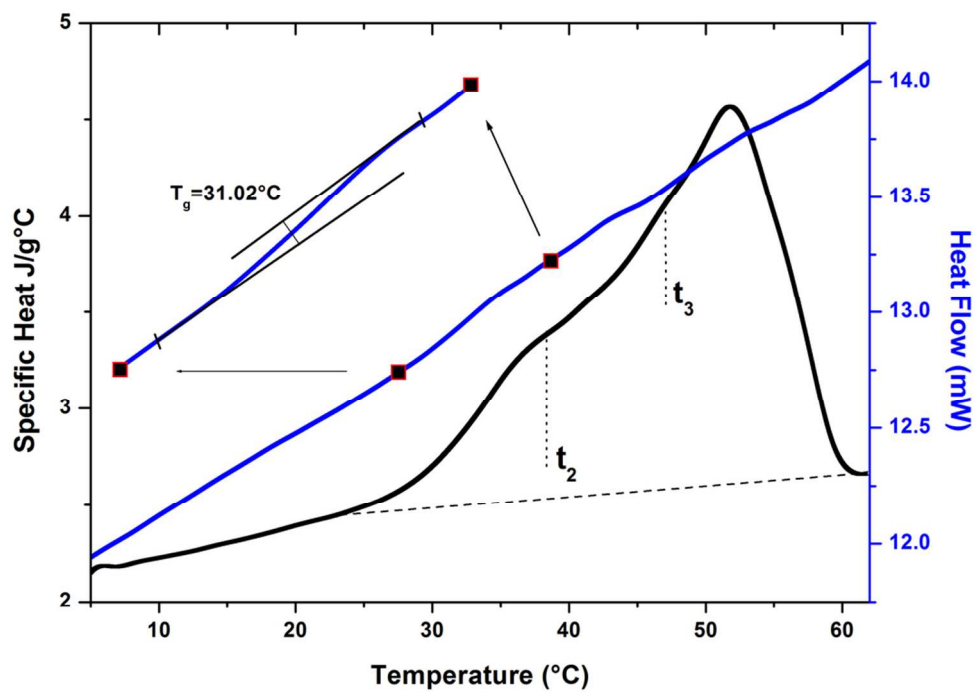
Figure 5: Nanoindentation curves obtained on the 75%wt for \dot{h}/h equal to 4, 0.4, 0.04 and 0.004 s^{-1} (a) and on pristine rosin for \dot{h}/h equal to 5, 0.5 and 0.05 s^{-1} (b).

Figure 6: Strain rate sensitivity as a function of the rosin content obtained from compression (m_{comp}), shear (m_{shear}) and nanoindentation (m_{nano}) tests.

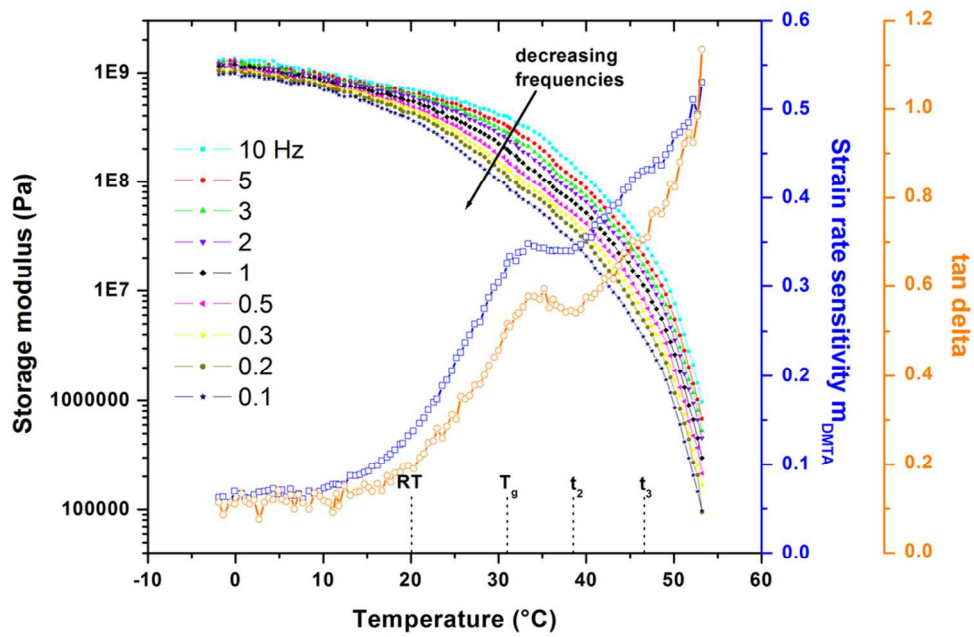
Graphical TOC: Strain rate sensitivity as a function of rosin content obtained from compression, shear and nanoindentation test performed in beeswax/rosin blends. In particular, a superplastic behaviour is clearly evidenced for blends containing more than 60%wt in rosin.



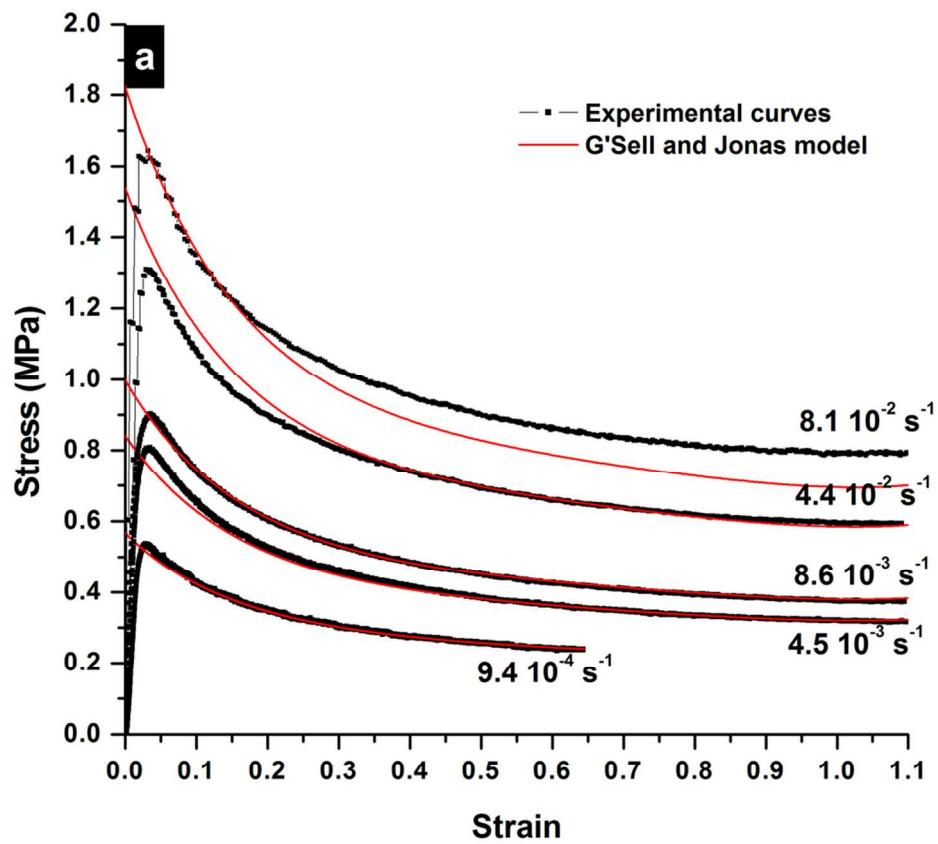
46x35mm (600 x 600 DPI)



46x33mm (600 x 600 DPI)

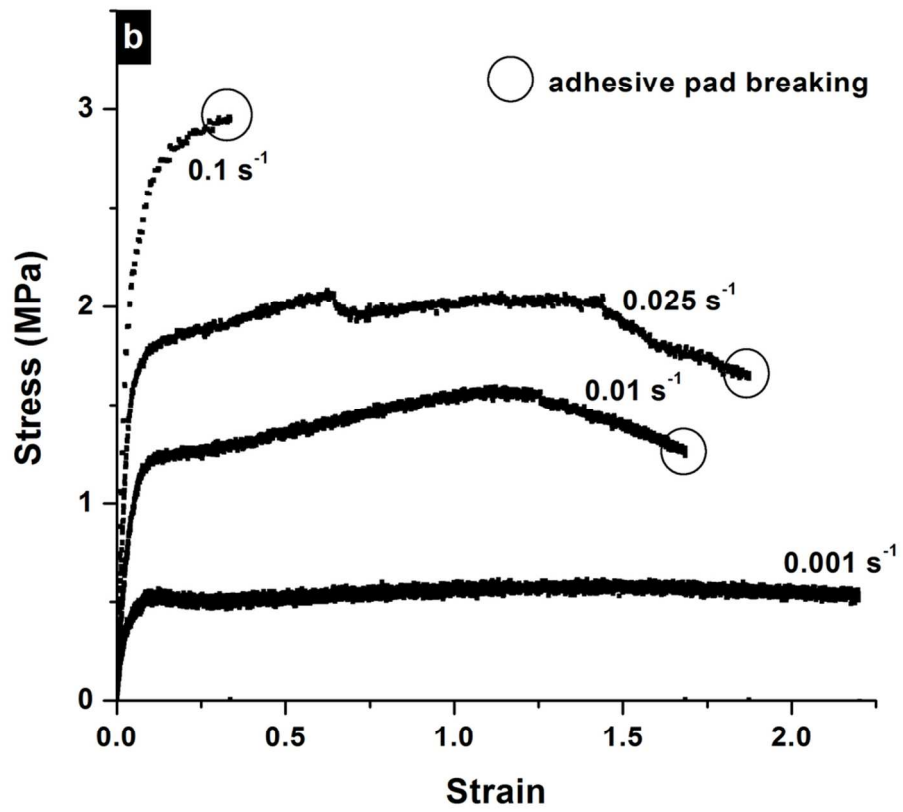


46x30mm (600 x 600 DPI)



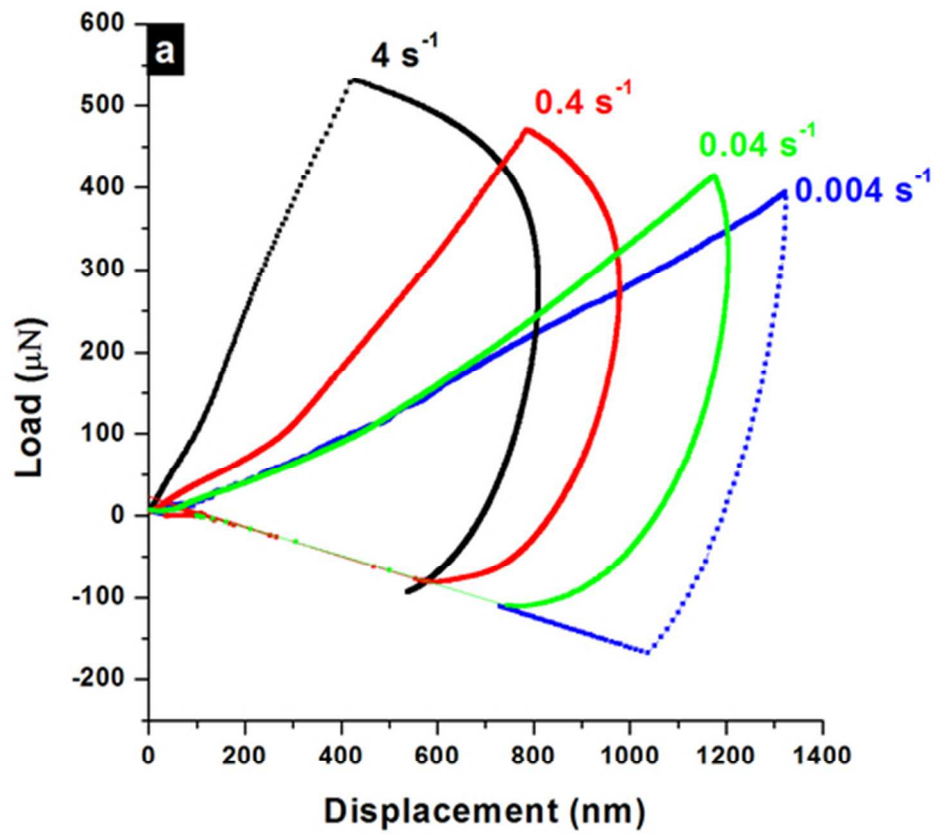
46x40mm (600 x 600 DPI)

iew

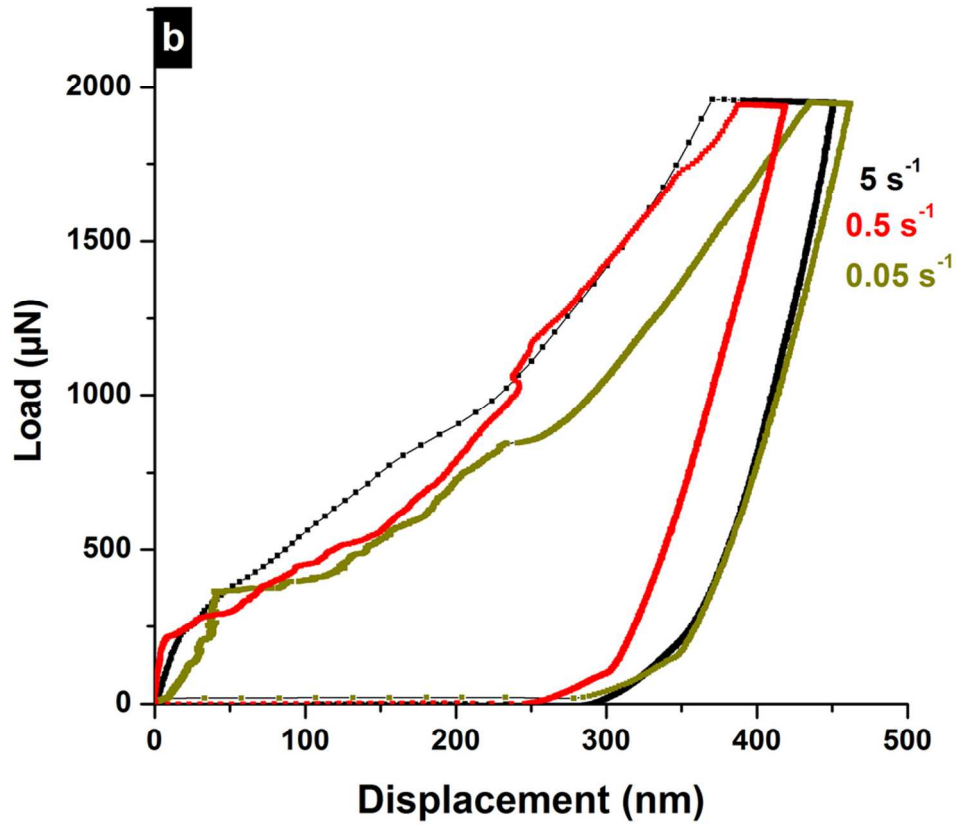


46x40mm (600 x 600 DPI)

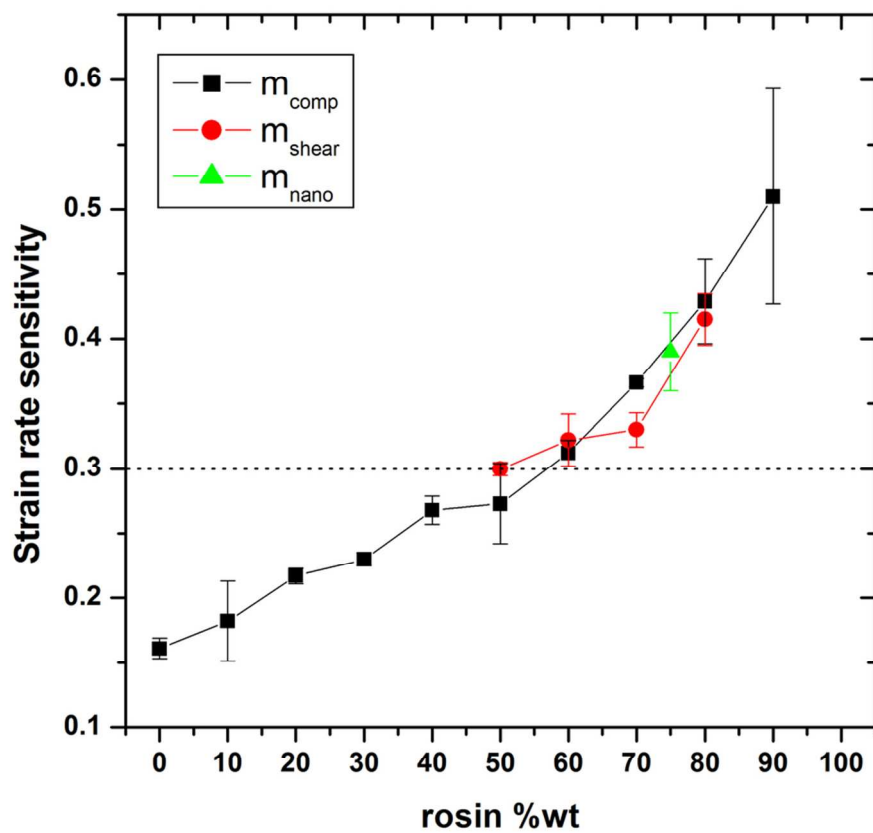
view



23x20mm (600 x 600 DPI)



45x38mm (600 x 600 DPI)



44x39mm (600 x 600 DPI)

iew